ACCOUNTS of chemical research

Article

Cite This: Acc. Chem. Res. 2018, 51, 950–959

pubs.acs.org/accounts

One-Dimensional Hetero-Nanostructures for Rechargeable Batteries

Liqiang Mai,* Jinzhi Sheng, Lin Xu, Shuangshuang Tan, and Jiashen Meng

State Key Laboratory of Advanced Technology for Materials Synthesis and Processing, International School of Materials Science and Engineering, Wuhan University of Technology, Wuhan, Hubei 430070, China

CONSPECTUS: Rechargeable batteries are regarded as one of the most practical electrochemical energy storage devices that are able to convert and store the electrical energy generated from renewable resources, and they function as the key power sources for electric vehicles and portable electronics. The ultimate goals for electrochemical energy storage devices are high power and energy density, long lifetime, and high safety. To achieve the above goals, researchers have tried to apply various morphologies of nanomaterials as the electrodes to enhance the electrochemical performance. Among them, one-dimensional (1D) materials show unique superiorities, such as cross-linked structures for external stress buffering and large draw ratios for internal stress dispersion. However, a homogeneous single-component electrode material can hardly have the characteristics of high electronic/ionic conductivity and high stability in the electrochemical environment simultaneously. Therefore, designing well-defined functional 1D hetero-nanostructures that combine the advantages and overcome the limitations of different electrochemically active materials is of great significance.

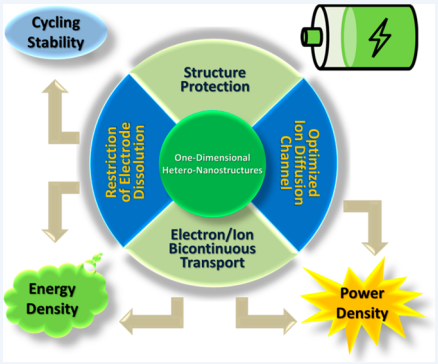

This Account summarizes fabrication strategies for 1D hetero-nanostructures, including nucleation and growth, deposition, and melt-casting and electrospinning. Besides, the chemical principles for each strategy are discussed. The nucleation and growth strategy is suitable for growing and constructing 1D hetero-nanostructures of partial transition metal compounds, and the experimental conditions for this strategy are relatively accessible. Deposition is a reliable strategy to synthesize 1D hetero-nanostructures by decorating functional layers on 1D substrate materials, on the condition that the preobtained substrate materials must be stable in the following deposition process. The melt-casting strategy, in which 1D hetero-nanostructures are synthesizes via a melting and molding process, is also widely used. Additionally, the main functions of 1D hetero-nanostructures are summarized into four aspects and reviewed in detail. Appropriate surface modification can effectively restrain the structure deterioration and the regeneration of the solid−electrolyte interphase layer caused by the volume change. A porous or semihollow external conducting material coating provides advanced electron/ion bicontinuous transmission. Suitable atomic heterogeneity in the crystal structure is beneficial to the expansion and stabilization of the ion diffusion channels. Multiphase-assisted structural design is also an accessible way for the sulfur electrode material restriction. Moreover, some outlooks about the further industrial production, more effective and cheaper fabrication strategies, and new heterostructures with smaller-scale composition are given in the last part. By providing an overview of fabrication methods and performance-enhancing mechanisms of 1D hetero-nanostructured electrode materials, we hope to pave a new way to facile and efficient construction of 1D hetero-nanostructures with practical utility.

1. INTRODUCTION

Since lithium ion batteries (LIBs) were commercialized by Sony in 1991, "rocking chair"-type batteries have undergone unprecedentedly rapid development in recent decades.[1−3] To meet the increasing demand for the functions of portable digital products, electric vehicles, and grid energy storage systems, researchers have used a variety of methods to improve the performance of these batteries.[4,5] As is well-known, the key factor of battery performance is the ability of electrodes to store metal cations.[4,5] The factors that influence the (dis)charge time (τ) are displayed in eq 1:[6]

$$\tau = \frac{L^2}{\alpha D} \quad (1)$$

where L is the average particle radius or half-thickness, α is a constant influenced by the materials parameters, and D is the effective chemical diffusivity of neutral lithium in the electrode materials. Thus, a shorter diffusion distance brings better (dis)charging rate capability. To pursue the essential advantages such as large electrode/electrolyte contact area and shortened ion diffusion paths, nanosized electrode materials have become a research hotspot for a long time.[7−13]

Among those nanomaterials, one-dimensional (1D) materials exhibit particular superiorities. Their special structures, with widths of less than 100 nm and lengths of several millimeters, make them more suitable for application to electrochemical nanodevices because this structure is easier to fix onto a current collector (Figure 1a).[14−17] In addition, 1D nanomaterials are easier to use in constructing interlaced flexible membranes by

Received: January 31, 2018
Published: April 5, 2018

DOI: 10.1021/acs.accounts.8b00031
Acc. Chem. Res. 2018, 51, 950–959

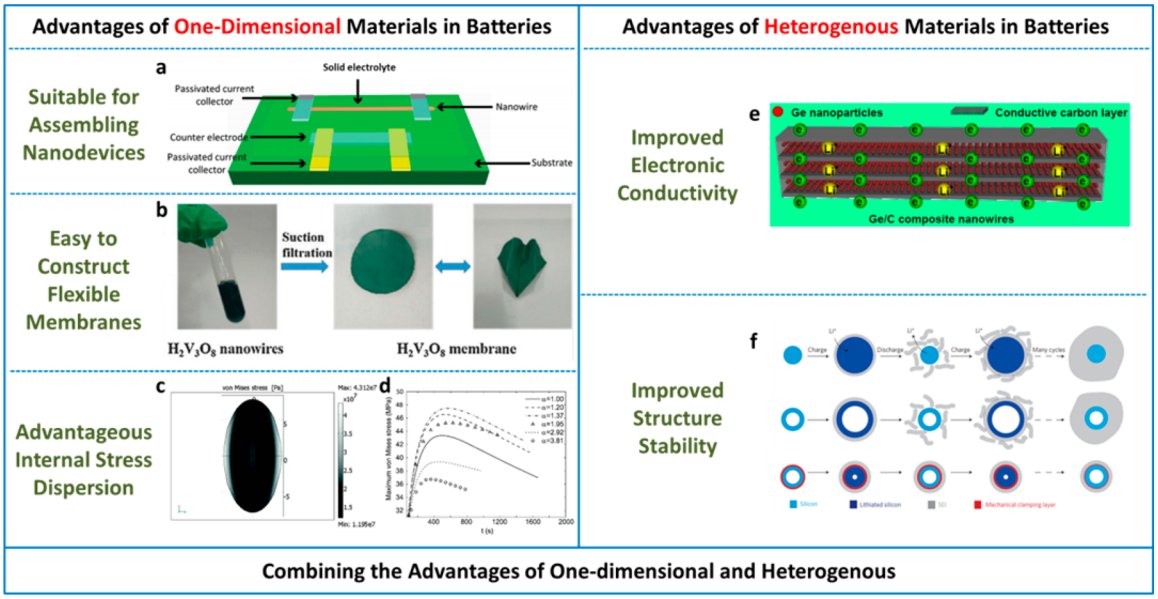

Figure 1. Advantages of one-dimensional and heterogeneous structures in energy storage. (a) Schematic diagram of a single nanowire electrode device design. (b) Nanowire membrane obtained via the suction filtration method. (c) Von Mises stress distribution in an ellipsoid with aspect ratio of 1.953 at the end of discharge. (d) Maximum von Mises stress during discharge for ellipsoids with various aspect ratios. (e) Schematic diagram of enhanced electron transport in the active material. (f) Schematic of the formation of a solid−electrolyte interphase on silicon surfaces. Panel (a) reproduced from ref 16. Copyright 2010 American Chemical Society. Panel (b) reproduced with permission from ref 19. Copyright 2016 the PCCP Owner Societies. Panels (c) and (d) reproduced with permission from ref 20. Copyright 2007 The Electrochemical Society. Panel (e) reproduced from ref 22. Copyright 2014 American Chemical Society. Panel (f) reproduced with permission from ref 10. Copyright 2012 Nature Publishing Group.

suction filtration, promoting the development of flexible energy storage devices (Figure 1b).[18,19] More importantly, for ion storage, 1D nanomaterials show unique structural stability. The stress distribution in the discharged elliptical particle was simulated, and it was found that the von Mises stress is larger around the equator (Figure 1c), which demonstrates that lathy structures could benefit the stress dispersion (Figure 1d).[20] Thus, 1D nanomaterials are regarded as promising and effective ion storage materials.

Although some materials were fabricated into 1D nanostructures, they still suffered from the typical drawbacks of most electrode materials. For instance, the intrinsic low electrical conductivity of some materials cannot be improved by changing their morphologies (Figure 1e).[12,21] Besides, volume expansion still exists in some conversion and alloying reaction-based materials, even though they have been designed into 1D nanostructures (Figure 1f).[10,22] Moreover, some electrode materials, such as sulfur, tend to dissolve in the electrolyte, resulting in severe capacity fading.[23] To solve these problems, in recent years researchers have used various second phases to decorate bare 1D materials to obtain better electrochemical performances, and materials with coaxial or hierarchical 1D hetero-nanostructures have been fabricated.[24−31] In addition to the superiorities inherited from the 1D nanostructures, improved electrochemical kinetics and enhanced structure stability are also obtained via synergetic effects among multiple components.[24−26] Thus, synthesizing more advanced 1D hetero-nanostructures in a controlled manner is significant for developing better batteries.

In this Account, fabrication strategies of 1D hetero-nanostructures are introduced from three aspects: heterogeneous nucleation and growth, deposition, and melt-casting and electrospinning. The factors influencing the synthesis process and the chemical principles of each strategy are discussed in detail, aiming to inspire ideas for more advanced manufacturing of 1D hetero-nanostructures. In addition, the effects of heterogeneous structures require a deeper understanding, and the functions of 1D hetero-nanostructures are summarized and reviewed. By providing an overview of fabrication methods and performance-enhancing mechanisms of 1D hetero-nanostructured electrode materials, we hope to pave a new way to facile and efficient construction of 1D hetero-nanostructures with practical utility. Finally, on the basis of the summaries and discussions, some personal perspectives on the development tendency of 1D hetero-nanostructured electrodes for rechargeable batteries are included.

2. DESIGNS AND PREPARATIONS

For decades, 1D hetero-nanostructured materials have been studied and applied in various branches. More and more facile and effective synthetic methods have been developed in recent years. Typical examples of these strategies and the key points for regulating the structures are introduced in this section.

2.1. Nucleation and Growth

As a typical wet-chemistry method, nucleation and growth is widely used for material preparation. To prepare 1D hetero-nanostructured materials, heterogeneous nucleation and growth play an important role. When a solution is under a certain degree of supersaturation or able to obtain energy from the external environment, the precursor atoms in this solution will condense to form nuclei.[32] If the supersaturated solution already contains stable nuclei, new material tends to grow on the seed materials without another nucleation process. The growth direction of the overgrown material depends on the contact angle of lattices between the seed material and the overgrown material.[33] On the basis of the nucleation type, one-

DOI: 10.1021/acs.accounts.8b00031
Acc. Chem. Res. 2018, 51, 950−959

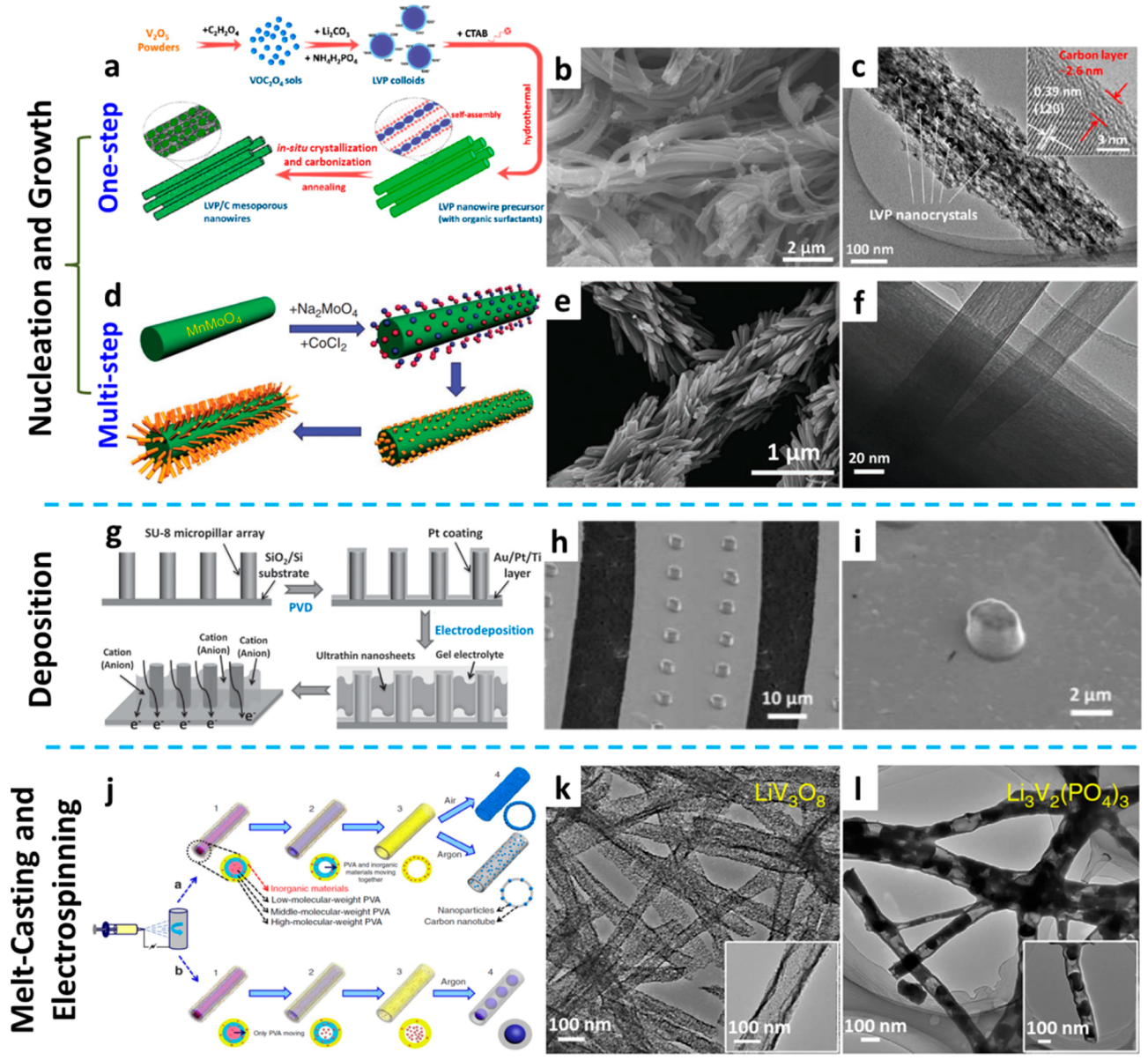

Figure 2. General synthetic methods for preparing 1D hetero-nanostructures. (a) Schematic illustration of the fabrication steps and proposed formation mechanism for the LVP/C-M-NWs. (b) SEM image of the LVP/C-M-NWs precursor. (c) TEM image of LVP/C-M-NWs. (d–f) Construction schematic diagram of hierarchical $MnMoO_4/CoMoO_4$ nanowires (d) and the related SEM (e) and TEM (f) images. (g) Schematic illustration of the fabrication process of SST-MPCs. (h) SEM image of the micropillar array coated by Pt. (i) SEM image of the array after electrodeposition. (j–l) Schematics of the gradient electrospinning and controlled pyrolysis methods (j) and TEM images of the heterogeneous LiV_3O_8/C (k) and $Li_3V_2(PO_4)_3/C$ (l) nanowires. Panels (a–c) reproduced from ref 27. Copyright 2014 American Chemical Society. Panels (d–f) reproduced with permission from ref 34. Copyright 2011 Nature Publishing Group. Panels (g–i) reproduced with permission from ref 36. Copyright 2015 John Wiley and Sons. Panels (j–l) reproduced with permission from ref 41. Copyright 2015 Nature Publishing Group.

step and multistep synthesis methods have been developed to fabricate various 1D hetero-nanostructures.

When different nuclei form synchronously, multiple phases tend to be evenly distributed in the structure, preferring a one-step growth process. For example, $Li_3V_2(PO_4)_3$/carbon mesoporous nanowires (LVP/C-M-NWs) were fabricated by the one-step hydrothermal method (Figure 2a), which is an effective way to obtain enough nucleation energy from the external environment.[27] The raw salts and surfactant were mixed in deionized water to form a $Li_3V_2(PO_4)_3$ homogeneous colloid, in which the nuclei were formed and the initial growth took place. Then the colloid solution was reacted under hydrothermal conditions to grow the nanowire precursor (Figure 2b), while the organics from the surfactant were composited in the nanowires. After crystallization of $Li_3V_2(PO_4)_3$ and carbonization of the organics through annealing, the LVP/C-M-NWs were formed (Figure 2c).

In many cases, the heterogeneous nucleation reaction may not be as harmonious as the above example. If the nuclei form severally and the prefabricated backbone material can remain stable under the following second-phase growthe environment, for better control of the morphology the growth processes had better take place one by one. Our group designed and fabricated hierarchical $MnMoO_4/CoMoO_4$ heterostructured nanowires using a two-step nucleation and growth process (Figure 2d–f).[34] The $MnMoO_4$ nanowire seed material was

DOI: 10.1021/acs.accounts.8b00031
Acc. Chem. Res. 2018, 51, 950–959

prepared by a simple microemulsion method and dispersed with $CoCl_2$ and Na_2MoO_4 in a supersaturated solution, in which the $CoMoO_4$ self-assembled on the $MnMoO_4$ nanowires to minimize the surface energy. $CoMoO_4$ continued to grow along the $CoMoO_4$ small crystals to form a hierarchical 1D structure. During this synthesis process, $CoMoO_4$ nuclei were easily formed and loaded on the surface of the $MnMoO_4$ nanowires with moderate outside conditions. The crystallographic orientation depends on the characteristics of the materials themselves. It is worth mentioning that some transition metal oxides (especially in the presence of elements such as V, Mo, Ti, Mn, Co, and so on) are more facile to grow along one certain direction.[24−28] The advantage of this strategy is the relatively accessible experimental conditions. However, obtaining homogeneous and small-sized morphologies requires multiple attempts to find the appropriate reaction conditions and experimental parameters.

2.2. Deposition

As we know, not all substances can be obtained by nucleation and growth in solutions. Also, uniformity of the morphologies and contact between different phases can hardly be ensured by chemical reactions without elaborate design. Common deposition methods, such as chemical vapor deposition (CVD), physical vapor deposition (PVD), and atomic layer deposition (ALD), are effective ways to finely coat functional materials on backbones to fabricate various coaxial 1D heterostructures. To carry out a deposition process, the substrates or the template materials need to be obtained primarily. CVD is usually used to coat carbon- and silicon-based structures on the surface of the substrates. When the gas molecules that participate in reactions are physically adsorbed on the surface of the substrate, the reaction starts and the crystal nuclei are formed. In contrast to heterogeneous nucleation, this process occurs in a gaseous environment and is a spontaneous chemical reaction, where the energy barriers that must be overcome are not very high. Compared with CVD, implementing ALD requires that the gas-phase precursors can be chemically adsorbed on the surface of the basis material. Nguyen et al.[35] fabricated alumina-coated silicon-based nanowire arrays via a multistep deposition process combining plasma-enhanced chemical vapor deposition (PECVD) and ALD. Briefly, silane (SiH_4) was introduced with a flow of H_2 to deposit on a nickel foam substrate, and $NiSi_x$ nanowires were grown. Then SiH_4 was sequentially deposited to form an α-Si layer on the surface of the $NiSi_x$ nanowires. Finally, trimethylaluminum and water were chosen as precursors, and the $NiSi_x$−α-Si nanowires with an Al_2O_3 coating were obtained via an ALD process.

Obviously, there are high requirements for the cost of experimental facilities when implementing the methods mentioned above. Except for those methods, electrodeposition and sputtering are the other two deposition techniques, which are relatively more accessible. Our group constructed all-solid-state spiral-shaped three-dimensional microcapacitors (SST-MPCs) through a multistep deposition process (Figure 2g).[36] First, an SU-8 micropillar array was directly fabricated by the electron-beam lithography technique. Then the Pt surface layer was deposited by PVD, and the obtained micropillar array is shown in Figure 2h. Afterward, ultrathin cobalt hydroxide and manganese dioxide nanosheets were electrodeposited on the 3D current collectors in the $Co(NO_3)_2{\cdot}6H_2O$ solution (Figure 2i). The substances of the coated layer, such as α-Si, Al_2O_3, and Pt, always can hardly be uniformly grown on other substrates via nucleation and growth but are stable in the monodisperse state. Thus, deposition is a reliable strategy to synthesize 1D hetero-nanostructures by decorating functional layers on 1D substrate materials, on the condition that the preobtained substrate materials must be stable in the following deposition process.

2.3. Melt-Casting and Electrospinning

The above-mentioned fabrication methods for 1D hetero-nanostructures, such as liquid nucleation growth and deposition methods, could be regarded as "inside-out" strategies, which rely on delicate chemical reactions. In contrast, the "outside-in" manufacturing method, known as "melt-casting", is also widely used to synthesize 1D heterostructures via a melting and molding process. For the casting process, nanosized templates with a 1D porous channel usually need to be provided. For example, an anodic aluminum oxide (AAO) membrane is one of the most typical templates. Many 1D alloy and nonmetallic heterogeneous nanowires have been synthesized using it as a template, assisted by a melt-casting process. Zheng et al.[30] designed a hollow sulfur/carbon (S/C) core/shell nanofiber via polystyrene carbonization, sulfur infusion, and an AAO etching process. The carbon nanotube shell is usually obtained using high-temperature carbonization of the organic or CVD.[37] Then molten sulfur is incorporated into the carbon nanotubes by heating the S/C mixture, which facilitates infiltration of molten sulfur onto the internal surface of the carbon nanotubes. Besides, SBA-15 and CMK-3 are widely used as templates to construct 1D heterogeneous nanostructures via similar melt/evaporation-casting or solvent evaporation-annealing methods, such as amorphous red phosphorus embedded on ordered mesoporous carbon[38] and mesoporous Si@carbon core−shell nanowires.[39] This strategy was also used for molten lithium infusion into porous nonconductive core/shell polyimide/ZnO matrix nanowires.[40]

Electrospinning is also a process of solidifying liquid materials to form wire morphologies, which can be regarded as a general method to fabricate nanowires. For instance, our group constructed layer-distributed nanowires by mixing low-, middle-, and high-molecular-weight poly(vinyl alcohol) (PVA) and inorganic salts in the precursor solution for electrospinning (Figure 2j−l).[41] During the heating treatment, PVA with different molecular weights was pyrolyzed in turn, carrying with it inorganic salts. After annealing in argon, the polymer was carbonized to form a carbon nanotube skeleton, on which the crystallized inorganic nanoparticles were attached with mesoporous structures. Generally, electrospinning as a progressive method has several advantages. For instance, length and thickness can be adjusted by changing the reaction parameters, and the component and concentration of the precursor solution can also be controlled to form 1D morphologies with different secondary structures. With the electrospinning apparatus being continuously improved, this method may be popularized, and the samples may be produced on a larger scale.

3. MODIFICATIONS AND APPLICATIONS

To this day, rechargeable batteries still suffer from some drawbacks such as insufficient capacity, low charge rate, capacity fading, and so on. These electrochemical performances mainly depend on the side reactions in the electrode materials. Constructing functional heterostructures always solves some of

DOI: 10.1021/acs.accounts.8b00031
Acc. Chem. Res. 2018, 51, 950−959

the stubborn but significant problems that severely restrict the further development of rechargeable batteries. In this section, mechanisms of four typical situations in which 1D hetero-nanostructures improve the electrochemical performance are summarized and introduced in detail.

3.1. Structure Protection

The electrode materials for rechargeable batteries are usually divided into intercalation, conversion, and alloying reaction mechanisms. The ion storage process is always accompanied by a nonnegligible volume change, especially in the latter two reactions.[10] In many battery systems, volume change is one of the culprits leading to sharp capacity fading. For instance, after reaction with Li^+, ~300% volume expansion occurs in SnO_2.[42] The volume expansion may give rise to serious structural degradation, which blocks the continuous ion transmission. Building stabilizing layers on the surface of active materials is necessary for a repeated expansion/shrink process, especially for alloying materials. For example, heterogeneous branched core−shell SnO_2−PANI nanorod arrays show much better structure stability than bare SnO_2 nanorods (Figure 3a).[42] The strong adhesion between the nanorod core and the conducting polymer shell provides mechanical integrity, and the excessive volume expansion after cycles is inhibited by the interaction between the branches, as confirmed by TEM results (Figure 3b,c). Other conducting polymers, such as PEDOT, were used to stabilize V_2O_5 nanowires,[21] and a carbon layer could also keep TiO_2 nanowires stable.[24] It should be noted that the decoration layer must have high electron and ion conductivity.

Large volume changes may also lead to breakup of the solid−electrolyte interphase (SEI) layer formed on the surface of the anode materials at low potential, and a new SEI layer tends to be regenerated, which irreversibly consumes lots of cations, resulting in low Coulombic efficiency in the initial cycles. To solve this problem in manganese oxide, yolk−shell nanorods with a manganese oxide core and carbon shell were constructed by our group via a sol−gel method.[43] The bare nanorods suffer repeated breaking and formation of the SEI layer during cycling, leading to thick SEI layers (Figure 3d). The cycling performance shows very low capacity of the bare nanorod from the second cycle, in stark contrast with the yolk−shell sample (Figure 3e). After cycling, the impedance of the bare nanorods increases obviously, mainly because of the formation of thick SEI layers (Figure 3f). Oppositely, the decreased charge transfer resistance of the yolk−shell sample indicates the activation and improved kinetics of the reaction, further demonstrating the enhanced structural stability. For instance, Wu et al.[10] designed a double-walled Si−SiO_x nanotube, in which the mechanical SiO_x outer wall enables the formation of a stable SEI. Meanwhile, the hollow void accommodates free volume expansion/constriction of the silicon without mechanical breaking. These designs take advantage of the confined effect of a mechanical clamping layer combined with the stress buffer of the unique 1D structure, effectively limiting the fracture and loss of active materials and improving the reaction kinetics, further realizing stable and fast ion storage.

3.2. Electron/Ion Bicontinuous Transport

As is well-known, most electrode materials suffer from poor electrical conductivity, resulting in low capacity and low rate capability. Enhancing the electrical conductivity of electrode materials is undoubtedly an important research direction for battery development. Coating conductive layers, such as carbon materials and conducting polymers, on the active materials

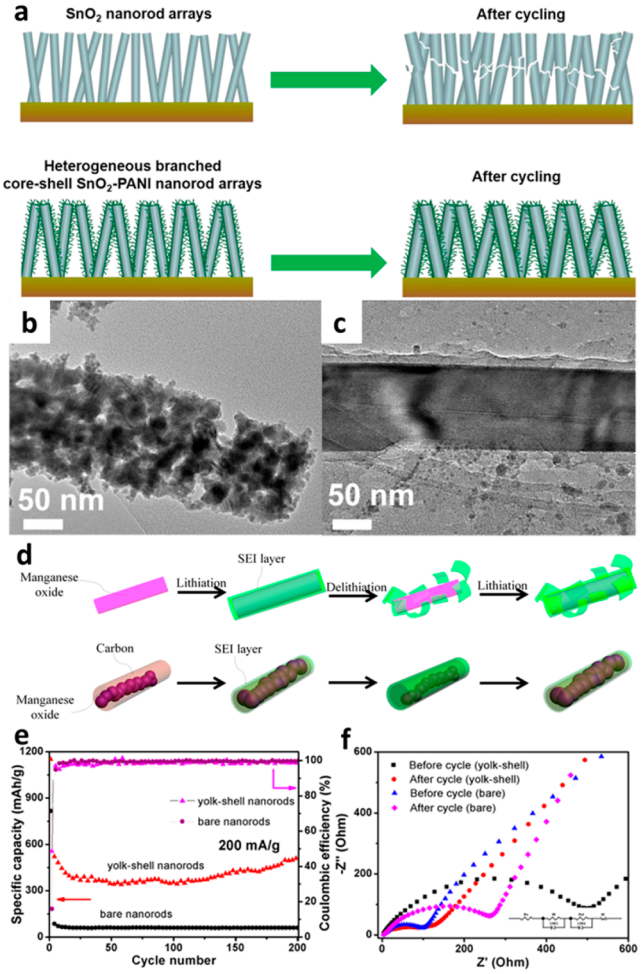

Figure 3. Typical examples of structure protection in 1D hetero-nanostructures. (a) Schematic illustrations of heterogeneous branched core−shell SnO_2−PANI nanorod arrays during cycling. (b, c) TEM images of bare SnO_2 nanorod arrays (b) and heterogeneous branched core−shell SnO_2−PANI nanorod arrays (c) after 40 cycles. (d) Three-dimensional views of a bare manganese oxide nanorod and a manganese oxide/carbon yolk−shell nanorod during lithiation and delithiation processes. (e) Cycling performances of yolk−shell nanorods and bare nanorods at 200 mA g^{-1}. (f) AC impedance plots for yolk−shell nanorods and bare nanorods before and after rate performance. Panels (a−c) reproduced with permission from ref 42. Copyright 2014 Elsevier. Panels (d−f) reproduced from ref 43. Copyright 2014 American Chemical Society.

becomes a common strategy to solve this problem. However, most of the electrically conductive layers are not favorable for ionic conduction. In the design of heterostructures with improved electrical conductivity, the ion transmission path should not be blocked. Structures that provide electron/ion bicontinuous transmission will be more advanced in ion storage. Our group designed single MnO_2/porous graphene oxide (MnO_2/pGO) wire-in-scroll electrochemical devices.[17] The introduction of pores in graphene not only improved the electrical conductivity of MnO_2 but also increased the ion diffusion coefficient (Figure 4a). The TEM image of the MnO_2/pGO nanowire shows hexagonal pores with a pore diameter of about 5 nm (Figure 4b). Compared with the MnO_2/pGO nanowire, the MnO_2/nonporous reduced graphene (MnO_2/rGO) sample exhibits lower capacitance at

DOI: 10.1021/acs.accounts.8b00031
Acc. Chem. Res. 2018, 51, 950−959

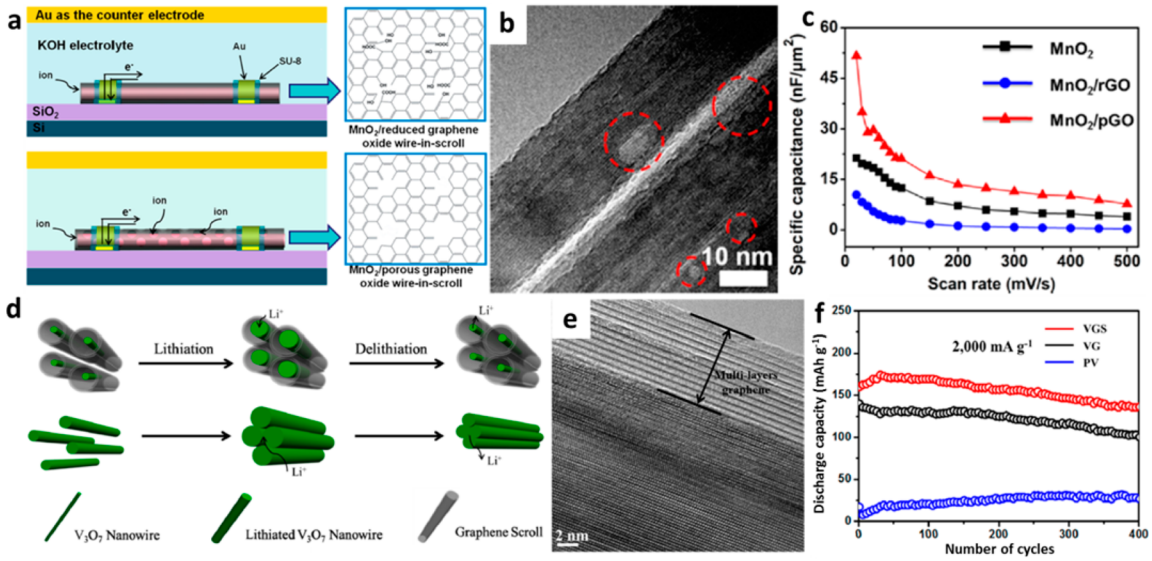

Figure 4. 1D hetero-nanostructures for electron/ion bicontinuous transmission. (a) Schematic illustrations of the MnO_2/rGO and MnO_2/pGO single nanowire devices. (b) HRTEM image of the edge of a MnO_2/pGO nanowire, showing pores in the material. (c) Plots of specific capacitance vs scan rate for MnO_2, MnO_2/rGO, and MnO_2/pGO single nanowire devices in 6 mol L^{-1} KOH. (d) Schematic of the V_3O_7 graphene scroll nanoarchitecture with continuous electron and Li ion transfer channels. (e) SEM image of the V_3O_7 graphene scrolls, showing the semihollow structure. (f) Galvanostatic discharge profiles of V_3O_7 graphene scrolls, V_3O_7 graphene composite, and pure V_3O_7 nanowires at 2.0 A g^{-1} tested between 4 and 1.5 V. Panels (a–c) reproduced from ref 17. Copyright 2016 American Chemical Society. Panels (d–f) reproduced from ref 25. Copyright 2013 American Chemical Society.

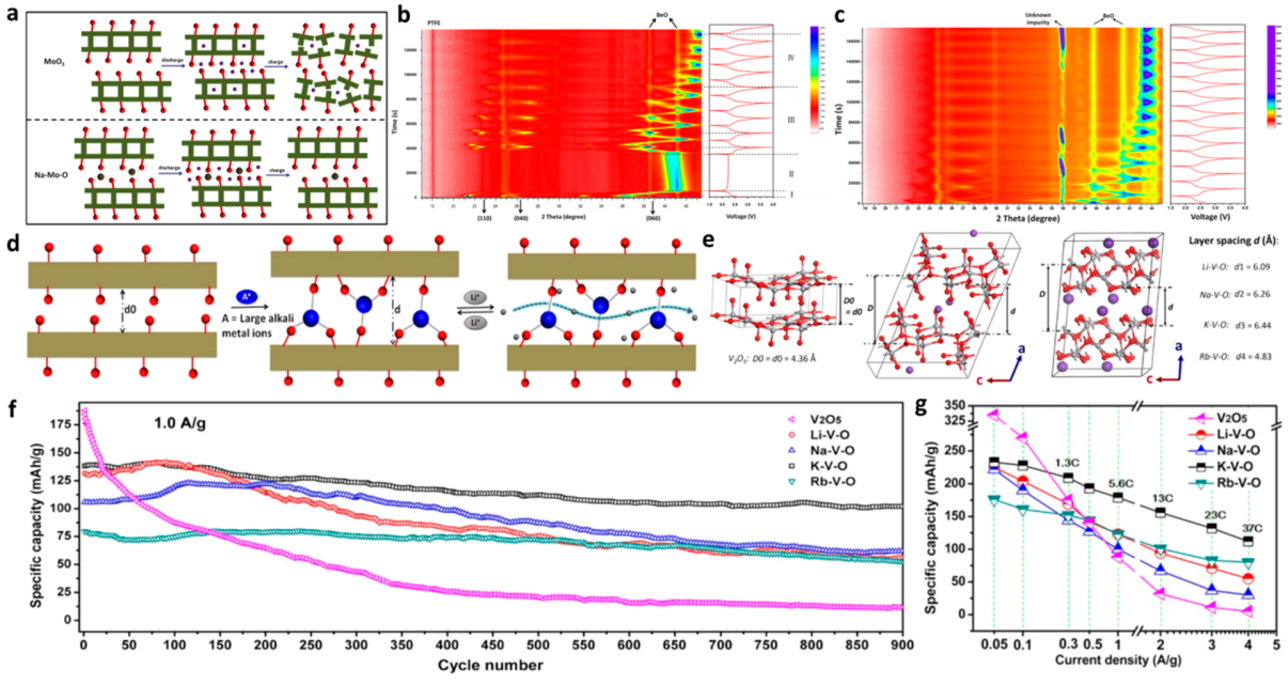

Figure 5. Atomic 1D heterostructures for expanded and stabilized ion diffusion channels. (a) Schematic illustration of the lithium intercalation/deintercalation process of MoO_3 and Na–Mo–O for the initial cycles. (b, c) In situ XRD patterns of Na^+-preintercalated MoO_3 (b) and pristine MoO_3 (c) for the initial cycles. (d) Schematic representation of large alkali metal ion intercalation. (e) Illustration of the crystal structures of (left to right) V_2O_5, A-V_6O_{15} (A = Li, Na, K), and RbV_3O_8. (f) Cycling performance of A–V–O nanowires at a charge/discharge rate of 1.0 A g^{-1}. (g) Rate performances of A–V–O nanowires. Panels (a–c) reproduced with permission from ref 44. Copyright 2015 Elsevier. Panels (d–g) reproduced from ref 45. Copyright 2015 American Chemical Society.

different scan rates (Figure 4c) because of the shielding effect of its decreased ion diffusion coefficient.

Although pores in the graphene provide channels for ion diffusion without degrading the rate of electron transport, the contact area between the electrode material and the electrolyte is still very limited. Thus, our group put forward another design to construct the semihollow coaxial structure as a pioneer that may substantially increase the active ion diffusion sites. For this purpose, a kind of V_3O_7-nanowire-templated semihollow bicontinuous graphene scroll architecture was fabricated

DOI: 10.1021/acs.accounts.8b00031
Acc. Chem. Res. 2018, 51, 950–959

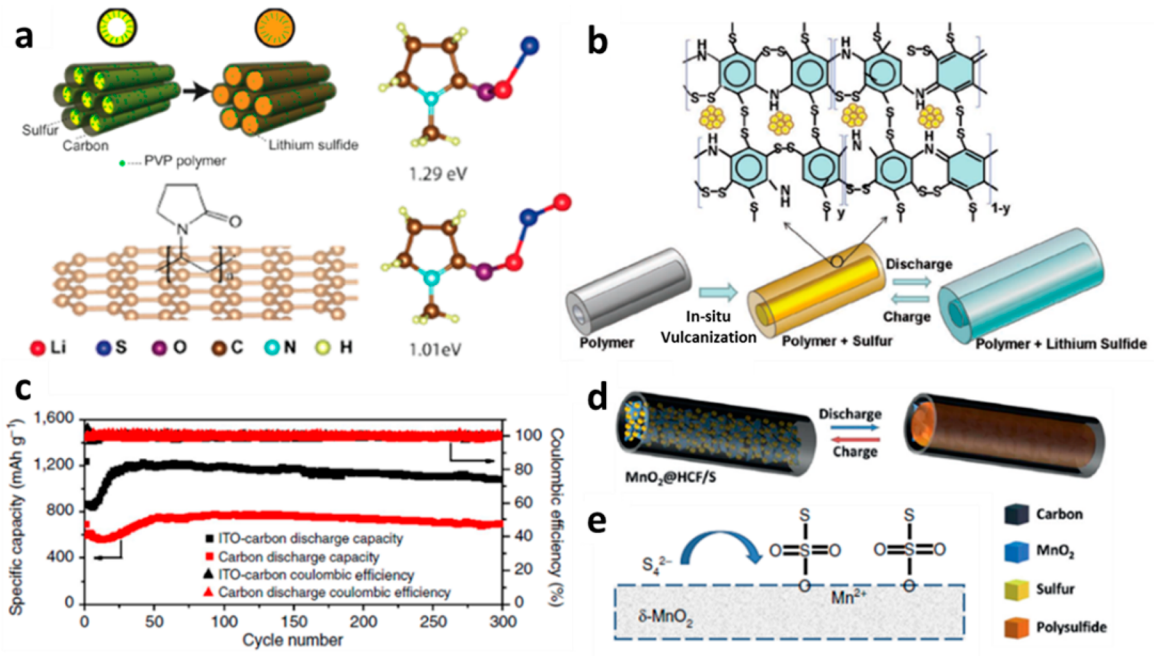

Figure 6. 1D heterostructures for sulfur restriction. (a) Schematic of polymer-modified sulfur encapsulated in a carbon nanotube cathode and corresponding first-principles calculation of the bonding energy between the discharge products and the functional group on the polymer. (b) Schematic of the structure and discharge−charge process of the SPANI-NT/S composite. (c) Discharge capacity and Coulombic efficiency of ITO−C hybrid nanofiber electrodes at C/5. (d) Schematic of the MnO_2@HCF/S electrode before (left) and after discharge (right). (e) Mechanism showing the formation of thiosulfate on the surface of MnO_2 by oxidation of initially formed polysulfide, concomitant with the reduction of Mn^{4+} to Mn^{2+}. Panel (a) reproduced from ref 47. Copyright 2013 American Chemical Society. Panel (b) reproduced with permission from ref 48. Copyright 2012 John Wiley & Sons. Panel (c) reproduced with permission from ref 49. Copyright 2014 Nature Publishing Group. Panel (d) reproduced with permission from ref 50. Copyright 2015 John Wiley & Sons, Inc. Panel (e) reproduced with permission from ref 51. Copyright 2015 Nature Publishing Group.

through an "oriented assembly and self-scroll" strategy.[25] The SEM image shows the clear semihollow structure (Figure 4e), in which the electrolyte can infiltrate into the graphene layer and better contact with the active material. In addition, the semihollow structure provides a buffer space for volume expansion when Li^+ is intercalated (Figure 4d). From the cycling performances (Figure 4f), the semihollow bicontinuous V_3O_7 nanowire/graphene sample (VGS) exhibits higher capacity than the ordinarily coated V_3O_7 nanowire/graphene sample (VG) and the pure V_3O_7 nanowire sample (PV). Compared with the samples tightly packed by the conductive layer, the samples with enough contact area to the electrolyte show better electrochemical performances. These results demonstrate that it is important to ensure unobstructed ion transmission paths while improving the electrical conductivity.

3.3. Expanded and Stabilized Ion Diffusion Channel by Atomic Heterogeneity

In addition to common problems such as volume change and low conductivity, the challenges intercalation materials face are not just about the macroscopic problems on the outside. The ion storage process in most cathode materials is always dominated by the inside ion diffusion. The influence of the inside diffusion on the electrochemical kinetics is no less than that of the external problems. Improving the crystal structure stability and expanding the ion diffusion channels of the existing cathode materials are two main goals that can be achieved through constructing atomic heterogeneity. For example, the irreversible structure change of α-MoO_3 during the charge−discharge process always leads to its poor electrochemical performance.[44] Through Na^+ preintercalation, the Na^+ will bond with the one-fold oxygen atoms and act as pillars to stabilize the structure of α-MoO_3, as shown in Figure 5a.[44] In situ XRD patterns of the Na^+-preintercalated MoO_3 sample show that the (060) peak at around 38° shifts to lower angle during the first discharge process and returns back after charge, though the shift becomes irreversible after several cycles (Figure 5b). However, the same peak of the pristine MoO_3 sample does not return to the initial position in the first cycle (Figure 5c). From these results it can be inferred that partial Na^+ between the interlayers is extracted accompanied by the extraction of Li^+, but the pillaring effect of Na^+ is weakened and the layer spacing in the lithiated structure decreases after cycles. Although the improvement only works for cycles, the positive effect of this strategy is undeniable.

Compared with the above transient effect, our group chose vanadium-based nanowires as the object, using alkali metal ions (Li, Na, K, Rb) to intercalate into the materials (Figure 5d).[45] The unit cell parameters refined by Pawley fitting show that K−V−O provides the largest interlayer spacing, while the preintercalation of Rb destroyed the initial structure (Figure 5e). On the basis of electrochemical tests, diffraction characterization, and calculations, it was found that the appropriate alkali metal ion intercalation in the admissible layered structure can avoid structure collapse, resulting in enhanced cyclability (Figure 5f). In addition, the expanded lattice distance also benefits the rate capability (Figure 5g). Pomerantseva and Gogotsi[46] also regarded this strategy of chemical preintercalation of inorganic ions as another method that can improve stability in cycle life tests. The above works confirm that constructing atomic heterogeneity is an effective strategy that fundamentally improves the properties of materials by changing

DOI: 10.1021/acs.accounts.8b00031
Acc. Chem. Res. 2018, 51, 950−959

the internal chemical bonds in the crystal. It has great potential for stabilizing and expanding the diffusion channels and developing electrodes with high energy and power density.

3.4. Restriction of Electrode Dissolution

High-energy-density Li−S batteries are being intensively studied for next-generation energy storage systems, but sulfur cathodes are limited by several factors, such as dissolution of polysulfide, the "shutting effect", and poor conductivity. The solutions for these issues largely depend on deep surface chemistry study and multiphase-assisted structural design. Modified 1D carbon hosts with −OH groups or N/S doping were designed to reduce dissolution of polysulfide through polar−polar interactions based on polar surfaces. Zheng et al.[47] introduced amphiphilic poly(vinylpyrrolidone) (PVP) to modify the surface of carbon nanotubes, rendering strong interactions between carbon surfaces and the polar Li_xS clusters (Figure 6a). Xiao et al.[48] used polyaniline (PAN) nanotubes to realize sulfur encapsulation at the molecular level (Figure 6b). In the sulfur infusion process, a fraction of elemental sulfur reacts with PAN to form a cross-linked, structurally stable sulfur−polyaniline (SPANI-NT) backbone with both intra- and interchain disulfide bond interconnectivity. To achieve higher discharge capacity and cycling stability, metal oxides and sulfides with intrinsic network polarity were employed to encapsulate sulfur elements and more effectively control the adsorption and deposition of polysulfides.[49] Tin-doped indium oxide nanoparticles with polar surfaces could spatially control the nucleation and deposition of solid S/Li_2S species and enhance the redox kinetics of polysulfides, resulting in improved performance (Figure 6c).

Besides the polar−polar chemical interaction between hosts and polysulfide, some probable mediators could be formed to bind polysulfide and promote stable redox activity during the discharge process. For example, MnO_2@hollow carbon nanofibers (MnO_2@HCF) delivered a specific capacity of 1161 mA h g^{-1} at 0.05C and maintained stable cycling performance at 0.5C over 300 cycles (Figure 6d).[50] A new mechanism was presented by Liang et al.[51] and further verified in many oxide hosts. Insoluble thiosulfate ($S_2O_3^{2-}$) as the mediator would be formed on the MnO_2 surface, resulting from the redox reaction between the initially formed Li_2S_x ($4 \le x \le 8$) and MnO_2 at the beginning of discharge (Figure 6e). Further reduction produces polysulfides that could be immediately catenated to form intermediate polythionate complexes and shorter-chain polysulfides by nucleophilic attack of $S_2O_3^{2-}$. Yu and co-workers also designed polypyrrole−MnO_2 coaxial nanotubes that greatly restrain the shuttle effect of polysulfides through chemisorption.[52] Moreover, 1D heterogeneous nanostructures as sulfur hosts also reduce volume expansion and improve the electron conduction of active sulfur. For further commercial applications, increasing the sulfur cathode loading is crucial. Thus, utilizing the knitted advantages of 1D hetero-nanostructures to realize higher-density electrodes that simultaneously relieve polysulfide dissolution should be developed in the future.

4. CONCLUSIONS AND OUTLOOKS

In this Account, some effective fabrication strategies have been introduced, and the chemical principles of each method for controllable synthesis of 1D hetero-nanostructured materials have been clearly explained. Besides, some drawbacks of electrodes, such as the continuous formation of an SEI layer and the growth of Li dendrites, have been solved via different effects provided by constructed heterostructures. The mechanisms of these effects have been illustrated in detail and may provide theoretical bases for the breakthrough of developing better electrodes in the near future.

Although some research achievements have been obtained in constructing 1D hetero-nanostructured electrodes, the demand for high-performance batteries will be much higher in the future, which requires the ongoing advancement of electrode materials. Current research achievements are not sufficient to optimize these materials as mature products that can be commercialized. There is still room for large improvements in the development of better 1D hetero-nanostructured materials. First, the compositing degree of various materials presently remains at the macroscopic scale. The positive interactions take effect only at the interfaces between the different phases, while other positions do not benefit from modifications. Thus, if the substances can be composited at a molecular level, the modification efficiency may sharply increase. New fabrication strategies for constructing heterogeneous materials at a smaller scale must be explored and developed. Second, most fabrication strategies can be mass-produced only with difficulty, which limits the industrialization prospects of these materials. In the coming decades, researchers must explore more effective fabrication methods or improve equipment to realize the large-scale production of 1D hetero-nanostructured materials. Additionally, choosing appropriate fabrication strategies that are suitable for the corresponding materials is a shortcut to obtaining products in large quantities at low cost. Third, the mass loading of active materials in the composite structures must still be increased, especially in the electrodes of Li−S batteries. Developing novel hetero-nanostructures with high mass loading is also a significant research direction that will sharply enhance the energy density of the whole battery. Developing novel electrodes with advanced compositions and structures to solve the drawbacks will always be desired but still has a significant way to go.

AUTHOR INFORMATION

Corresponding Author

*E-mail: mlq518@whut.edu.cn (L. Mai).

ORCID

Liqiang Mai: 0000-0003-4259-7725

Notes

The authors declare no competing financial interest.

Biographies

Liqiang Mai is currently the Changjiang Scholar Chair Professor of Materials Science and Engineering at Wuhan University of Technology. He is mainly engaged in the research field of nano energy materials and micro/nano devices.

Jinzhi Sheng is currently a Ph.D. student at Wuhan University of Technology. His research interest is superionic conductor electrode materials for rechargeable batteries.

Lin Xu is currently a professor at Wuhan University of Technology. His research focuses on nano energy devices and nanobioelectronics.

Shuangshuang Tan is currently a Ph.D. student at Wuhan University of Technology. His current research focuses on sulfur-based energy storage materials and devices.

DOI: 10.1021/acs.accounts.8b00031
Acc. Chem. Res. 2018, 51, 950−959

Jiashen Meng is currently working toward a Ph.D. degree at Wuhan University of Technology, and his current research focuses on metal−organic framework materials for energy storage.

■ ACKNOWLEDGMENTS

This work was supported by the National Natural Science Fund for Distinguished Young Scholars (51425204), the National Natural Science Foundation of China (51602239), the National Key Research and Development Program of China (2016YFA0202603, 2016YFA0202601), the National Basic Research Program of China (2013CB934103), the Programme of Introducing Talents of Discipline to Universities (B17034), the Yellow Crane Talent (Science & Technology) Program of Wuhan City.

■ REFERENCES

(1) Van der Ven, A.; Bhattacharya, J.; Belak, A. A. Understanding Li Diffusion in Li-Intercalation Compounds. *Acc. Chem. Res.* **2013**, *46*, 1216−1225.
(2) Armand, M.; Tarascon, J. M. Building Better Batteries. *Nature* **2008**, *451*, 652−657.
(3) Shi, Y.; Zhou, X.; Yu, G. Material and Structural Design of Novel Binder Systems for High-Energy, High-Power Lithium-Ion Batteries. *Acc. Chem. Res.* **2017**, *50*, 2642−2652.
(4) Xia, H.; Wan, Y.; Assenmacher, W.; Mader, W.; Yuan, G.; Lu, L. Facile Synthesis of Chain-Like $LiCoO_2$ Nanowire Arrays as Three-Dimensional Cathode for Microbatteries. *NPG Asia Mater.* **2014**, *6*, e126.
(5) Augustyn, V.; Simon, P.; Dunn, B. Pseudocapacitive Oxide Materials for High-rate Electrochemical Energy Storage. *Energy Environ. Sci.* **2014**, *7*, 1597−1614.
(6) Zhu, C.; Usiskin, R. E.; Yu, Y.; Maier, J. The Nanoscale Circuitry of Battery Electrodes. *Science* **2017**, *358*, eaao2808.
(7) Poizot, P.; Laruelle, S.; Grugeon, S.; Dupont, L.; Tarascon, J.-M. Nano-Sized Transition-Metal Oxides as Negative-Electrode Materials for Lithium-Ion Batteries. *Nature* **2000**, *407*, 496−499.
(8) Li, G.; Luo, D.; Wang, X. L.; Seo, M. H.; Hemmati, S.; Yu, A. P.; Chen, Z. W. Enhanced Reversible Sodium-Ion Intercalation by Synergistic Coupling of Few-Layered MoS_2 and S-Doped Graphene. *Adv. Funct. Mater.* **2017**, *27*, 1702562.
(9) Xia, H.; Hong, C.; Shi, X.; Li, B.; Yuan, G.; Yao, Q.; Xie, J. Hierarchical Heterostructures of Ag Nanoparticles Decorated MnO_2 Nanowires as Promising Electrodes for Supercapacitors. *J. Mater. Chem. A* **2015**, *3*, 1216−1221.
(10) Wu, H.; Chan, G.; Choi, J. W.; Ryu, I.; Yao, Y.; McDowell, M. T.; Lee, S. W.; Jackson, A.; Yang, Y.; Hu, L. B.; Cui, Y. Stable Cycling of Double-walled Silicon Nanotube Battery Anodes Through Solid−electrolyte Interphase Control. *Nat. Nanotechnol.* **2012**, *7*, 310−315.
(11) Mai, L. Q.; Yan, M. Y.; Zhao, Y. L. Track batteries degrading in real time. *Nature* **2017**, *546*, 469−470.
(12) Zhao, Y.; Peng, L.; Liu, B.; Yu, G. Single-Crystalline $LiFePO_4$ Nanosheets for High-Rate Li-Ion Batteries. *Nano Lett.* **2014**, *14*, 2849−2853.
(13) Xia, H.; Xia, Q.; Lin, B.; Zhu, J.; Seo, J. K.; Meng, Y. S. Self-standing Porous $LiMn_2O_4$ Nanowall Arrays as Promising Cathodes for Advanced 3D Microbatteries and Flexible Lithium-ion Batteries. *Nano Energy* **2016**, *22*, 475−482.
(14) Mai, L. Q.; Tian, X.; Xu, X.; Chang, L.; Xu, L. Nanowire Electrodes for Electrochemical Energy Storage Devices. *Chem. Rev.* **2014**, *114*, 11828−11862.
(15) Kong, Q.; Kim, D.; Liu, C.; Yu, Y.; Su, Y.; Li, Y. F.; Yang, P. D. Directed Assembly of Nanoparticle Catalysts on Nanowire Photoelectrodes for Photoelectrochemical CO_2 Reduction. *Nano Lett.* **2016**, *16*, 5675−5680.
(16) Mai, L. Q.; Dong, Y. J.; Xu, L.; Han, C. Single Nanowire Electrochemical Devices. *Nano Lett.* **2010**, *10*, 4273−4278.
(17) Hu, P.; Yan, M. Y.; Wang, X. P.; Han, C. H.; He, L.; Wei, X. J.; Niu, C. J.; Zhao, K. N.; Tian, X. C.; Wei, Q. L.; Li, Z. J.; Mai, L. Q. Single-Nanowire Electrochemical Probe Detection for Internally Optimized Mechanism of Porous Graphene in Electrochemical Devices. *Nano Lett.* **2016**, *16*, 1523−1529.
(18) Xiong, C.; Aliev, A. E.; Gnade, B.; Balkus, K. J. Fabrication of Silver Vanadium Oxide and V_2O_5 Nanowires for Electrochromics. *ACS Nano* **2008**, *2*, 293−301.
(19) Wang, D.; Wei, Q. L.; Sheng, J. Z.; Hu, P.; Yan, M. Y.; Sun, R. M.; Xu, X. M.; An, Q. Y.; Mai, L. Q. Flexible Additive Free $H_2V_3O_8$ Nanowire Membrane as Cathode for Sodium Ion Batteries. *Phys. Chem. Chem. Phys.* **2016**, *18*, 12074−12079.
(20) Zhang, X.; Shyy, W.; Sastry, A. M. Numerical Simulation of Intercalation-Induced Stress in Li-Ion Battery Electrode Particles. *J. Electrochem. Soc.* **2007**, *154*, A910−A916.
(21) Mai, L. Q.; Dong, F.; Xu, X.; Luo, Y. Z.; An, Q. Y.; Zhao, Y. L.; Pan, J.; Yang, J. N. Cucumber-Like V_2O_5/poly(3,4-ethylenedioxythiophene)&MnO_2 Nanowires with Enhanced Electrochemical Cyclability. *Nano Lett.* **2013**, *13*, 740−745.
(22) Liu, J.; Song, K.; Zhu, C.; Chen, C. C.; van Aken, P. A.; Maier, J.; Yu, Y. Ge/C Nanowires as High-Capacity and Long-Life Anode Materials for Li-Ion Batteries. *ACS Nano* **2014**, *8*, 7051−7059.
(23) Zhao, F.; Shi, Y.; Pan, L.; Yu, G. Multifunctional Nanostructured Conductive Polymer Gels: Synthesis, Properties, and Applications. *Acc. Chem. Res.* **2017**, *50*, 1734−1743.
(24) Liao, J. Y.; Higgins, D.; Lui, G.; Chabot, V.; Xiao, X.; Chen, Z. Multifunctional TiO_2-C/MnO_2 Core-Double-Shell Nanowire Arrays as High-Performance 3D Electrodes for Lithium Ion Batteries. *Nano Lett.* **2013**, *13*, 5467−5473.
(25) Yan, M. Y.; Wang, F. C.; Han, C. H.; Ma, X. Y.; Xu, X.; An, Q. Y.; Xu, L.; Niu, C. J.; Zhao, Y. L.; Tian, X. C.; Hu, P.; Wu, H. G.; Mai, L. Q. Nanowire Templated Semihollow Bicontinuous Graphene Scrolls: Designed Construction, Mechanism, and Enhanced Energy Storage Performance. *J. Am. Chem. Soc.* **2013**, *135*, 18176−18182.
(26) An, Q. Y.; Lv, F.; Liu, Q. Q.; Han, C. H.; Zhao, K. N.; Sheng, J. Z.; Wei, Q. L.; Yan, M. Y.; Mai, L. Q. Amorphous Vanadium Oxide Matrixes Supporting Hierarchical Porous Fe_3O_4/Graphene Nanowires as a High-Rate Lithium Storage Anode. *Nano Lett.* **2014**, *14*, 6250−6256.
(27) Wei, Q. L.; An, Q. Y.; Chen, D. D.; Mai, L. Q.; Chen, S. Y.; Zhao, Y. L.; Hercule, K. M.; Xu, L.; Minhas-Khan, A.; Zhang, Q. J. One-Pot Synthesized Bicontinuous Hierarchical $Li_3V_2(PO_4)_3$/C Mesoporous Nanowires for High-Rate and Ultralong-Life Lithium-ion Batteries. *Nano Lett.* **2014**, *14*, 1042−1048.
(28) Wang, X. P.; Niu, C. J.; Meng, J. S.; Hu, P.; Xu, X. M.; Wei, X. J.; Zhou, L.; Zhao, K. N.; Luo, W.; Yan, M. Y.; Mai, L. Q. Novel $K_3V_2(PO_4)_3$/C Bundled Nanowires as Superior Sodium-Ion Battery Electrode with Ultrahigh Cycling Stability. *Adv. Energy Mater.* **2015**, *5*, 1500716.
(29) Liu, Y. Y.; Lin, D. C.; Liang, Z.; Zhao, J.; Yan, K.; Cui, Y. Lithium-coated Polymeric Matrix as a Minimum Volume-change and Dendrite-free Lithium Metal Anode. *Nat. Commun.* **2016**, *7*, 10992.
(30) Zheng, G.; Yang, Y.; Cha, J. J.; Hong, S. S.; Cui, Y. Hollow Carbon Nanofiber-Encapsulated Sulfur Cathodes for High Specific Capacity Rechargeable Lithium Batteries. *Nano Lett.* **2011**, *11*, 4462−4467.
(31) Chen, Y. M.; Yu, X. Y.; Li, Z.; Paik, U.; Lou, X. W. Hierarchical MoS2 Tubular Structures Internally Wired by Carbon Nanotubes as a Highly Stable Anode Material for Lithium-ion Batteries. *Sci. Adv.* **2016**, *2*, e1600021.
(32) Zhang, R.; Khalizov, A.; Wang, L.; Hu, M.; Xu, W. Nucleation and Growth of Nanoparticles in the Atmosphere. *Chem. Rev.* **2012**, *112*, 1957−2011.
(33) Sun, Y. G. Interfaced Heterogeneous Nanodimers. *Natl. Sci. Rev.* **2015**, *2*, 329−348.
(34) Mai, L. Q.; Yang, F.; Zhao, Y. L.; Xu, X.; Xu, L.; Luo, Y. Z. Hierarchical $MnMoO_4$/$CoMoO_4$ Heterostructured Nanowires with Enhanced Supercapacitor Performance. *Nat. Commun.* **2011**, *2*, 381.

DOI: 10.1021/acs.accounts.8b00031
Acc. Chem. Res. 2018, 51, 950−959

(35) Nguyen, H. T.; Zamfir, M. R.; Duong, L. D.; Lee, Y. H.; Bondavalli, P.; Pribat, D. Alumina-coated Silicon-based Nanowire Arrays for High Quality Li-ion Battery Anodes. *J. Mater. Chem.* **2012**, *22*, 24618−24626.
(36) Tian, X.; Shi, M.; Xu, X.; Yan, M.; Xu, L.; Minhas-Khan, K.; Han, C.; He, L.; Mai, L. Arbitrary Shape Engineerable Spiral Micropseudocapacitors with Ultrahigh Energy and Power Densities. *Adv. Mater.* **2015**, *27*, 7476−7482.
(37) Moon, S.; Jung, Y. H.; Jung, W. K.; Jung, D. S.; Choi, J. W.; Kim, D. K. Encapsulated Monoclinic Sulfur for Stable Cycling of Li−S Rechargeable Batteries. *Adv. Mater.* **2013**, *25*, 6547−6553.
(38) Li, W.; Yang, Z.; Li, M.; Jiang, Y.; Wei, X.; Zhong, X.; Gu, L.; Yu, Y. Amorphous Red Phosphorus Embedded in Highly Ordered Mesoporous Carbon with Superior Lithium and Sodium Storage Capacity. *Nano Lett.* **2016**, *16*, 1546−1553.
(39) Kim, H.; Cho, J. Superior Lithium Electroactive Mesoporous Si@Carbon Core-Shell Nanowires for Lithium Battery Anode Material. *Nano Lett.* **2008**, *8*, 3688−3691.
(40) Liu, Y.; Lin, D.; Liang, Z.; Zhao, J.; Yan, K.; Cui, Y. Lithium-coated Polymeric Matrix as a Minimum Volume-change and Dendrite-free Lithium Metal Anode. *Nat. Commun.* **2016**, *7*, 10992.
(41) Niu, C. J.; Meng, J. S.; Wang, X. P.; Han, C. H.; Yan, M. Y.; Zhao, K. N.; Xu, X. M.; Ren, W. H.; Zhao, Y. L.; Xu, L.; Zhang, Q. J.; Zhao, D. Y.; Mai, L. Q. General Synthesis of Complex Nanotubes by Gradient Electrospinning and Controlled Pyrolysis. *Nat. Commun.* **2015**, *6*, 7402.
(42) Xu, W. W.; Zhao, K. N.; Niu, C. J.; Zhang, L.; Cai, Z. Y.; Han, C. H.; He, L.; Shen, T.; Yan, M. Y.; Qu, L. B.; Mai, L. Q. Heterogeneous Branched Core−shell SnO_2-PANI Nanorod Arrays with Mechanical Integrity and Three Dimentional Electron Transport for Lithium Batteries. *Nano Energy* **2014**, *8*, 196−204.
(43) Cai, Z. Y.; Xu, L.; Yan, M. Y.; Han, C. H.; He, L.; Hercule, K. M.; Niu, C. J.; Yuan, Z. F.; Xu, W. W.; Qu, L. B.; Zhao, K. N.; Mai, L. Q. Manganese Oxide/carbon Yolk-shell Nanorod Anodes for High Capacity Lithium Batteries. *Nano Lett.* **2015**, *15*, 738−744.
(44) Dong, Y. F.; Xu, X. M.; Li, S.; Han, C. H.; Zhao, K. N.; Zhang, L.; Niu, C. J.; Huang, Z.; Mai, L. Q. Inhibiting Effect of Na^+ Pre-intercalation in MoO_3 Nanobelts with Enhanced Electrochemical Performance. *Nano Energy* **2015**, *15*, 145−152.
(45) Zhao, Y. L.; Han, C. H.; Yang, J. W.; Su, J.; Xu, X. M.; Li, S.; Xu, L.; Fang, R. P.; Jiang, H.; Zou, X. D.; Song, B.; Mai, L. Q.; Zhang, Q. J. Stable Alkali Metal Ion Intercalation Compounds as Optimized Metal Oxide Nanowire Cathodes for Lithium Batteries. *Nano Lett.* **2015**, *15*, 2180−2185.
(46) Pomerantseva, E.; Gogotsi, Y. Two-dimensional Heterostructures for Energy Storage. Nat. *Energy* **2017**, *2*, 17089.
(47) Zheng, G.; Zhang, Q.; Cha, J. J.; Yang, Y.; Li, W.; Seh, Z. W.; Cui, Y. Amphiphilic Surface Modification of Hollow Carbon Nanofibers for Improved Cycle Life of Lithium Sulfur Batteries. *Nano Lett.* **2013**, *13*, 1265−1270.
(48) Xiao, L.; Cao, Y.; Xiao, J.; Schwenzer, B.; Engelhard, M. H.; Saraf, L. V.; Nie, Z.; Exarhos, G. J.; Liu, J. A Soft Approach to Encapsulate Sulfur. *Adv. Mater.* **2012**, *24*, 1176−1181.
(49) Yao, H.; Zheng, G.; Hsu, P.-C.; Kong, D.; Cha, J. J.; Li, W.; Seh, Z. W.; McDowell, M. T.; Yan, K.; Liang, Z.; Narasimhan, V. K.; Cui, Y. Improving Lithium-Sulphur Batteries through Spatial Control of Sulphur Species Deposition on a Hybrid Electrode Surface. *Nat. Commun.* **2014**, *5*, 3943.
(50) Li, Z.; Zhang, J.; Lou, X. W. Hollow Carbon Nanofibers Filled with MnO_2 Nanosheets as Efficient Sulfur Hosts for Lithium-Sulfur Batteries. *Angew. Chem., Int. Ed.* **2015**, *54*, 12886.
(51) Liang, X.; Hart, C.; Pang, Q.; Garsuch, A.; Weiss, T.; Nazar, L. F. A Highly Efficient Polysulfide Mediator for Lithium-sulfur Batteries. *Nat. Commun.* **2015**, *6*, 5682.
(52) Zhang, J.; Shi, Y.; Ding, Y.; Zhang, W.; Yu, G. In Situ Reactive Synthesis of Polypyrrole-MnO_2 Coaxial Nanotubes as Sulfur Hosts for High-Performance Lithium-Sulfur Battery. *Nano Lett.* **2016**, *16*, 7276−7281.

DOI: 10.1021/acs.accounts.8b00031
Acc. Chem. Res. 2018, 51, 950−959